

Polarization and multiscale structural balance in signed networks

Szymon Talaga^{1*} Massimo Stella² Trevor James Swanson³
 Andreia Sofia Teixeira⁴

¹Robert Zajonc Institute for Social Studies, University of Warsaw,
 Stawki 5/7, 00-183 Warsaw, Poland.

²Dipartimento di Psicologia e Scienze Cognitive, University of Trento
 Corso Bettini 84, 38068, Rovereto (TN), Italy

⁴LASIGE and Departamento de Informática, Faculdade de Ciências, Universidade de Lisboa,
 Lisboa, Portugal

*Corresponding author; E-mail: stalaga@uw.edu.pl

Abstract

Polarization is a common feature of social systems. Structural Balance Theory studies polarization of positive in-group and negative out-group ties in terms of semicycles within signed networks. However, enumerating semicycles is computationally expensive, so approximations are often needed to assess balance. Here we introduce Multiscale Semiwalk Balance (MSB) approach for quantifying the degree of balance (DoB) in (un)directed, (un)weighted signed networks by approximating semicycles with closed semiwalks. MSB allows principled selection of a range of cycle lengths appropriate for assessing DoB and interpretable under the Locality Principle (which posits that patterns in shorter cycles are crucial for balance). This flexibility overcomes several limitations affecting walk-based approximations and enables efficient, interpretable methods for measuring DoB and clustering signed networks. We demonstrate the effectiveness of our approach by applying it to real-world social systems. For instance, our methods capture increasing polarization in the U.S. Congress, which may go undetected with other methods.

1. Introduction

Networks are used in many branches of science and engineering for modeling complex relational systems. Depending on properties of systems they represent, they may be undirected (ties are bidirectional) or directed and weighted (ties have weights which usually indicate strength) or unweighted [37]. A particular variant are signed networks, in which ties are either positive or negative and so can be used to model valenced relations such as liking and disliking or alliances and war [9, 10, 23, 50]. Signed networks are commonly used for representing systems capable of polarization, or clustering into groups with positive in-group and negative out-group ties. As a result, they have long been important to social scientists interested in polarization and differentiation processes inherent to formation of groups, attitudes and opinions [7, 9, 36, 45, 54]. However, signed networks are also used in other disciplines for modeling diverse phenomena such as brain activation [42],

ecological interactions [43], and financial time series [14]. Moreover, it is often not only the signs that matter, but also the weights indicating intensities of particular relations. Therefore, principled methods for analyzing signed networks, possibly with weights, are important for many applications.

Since signed networks represent valenced relations, a fundamental question concerns the degree to which positive and negative ties are consistent with respect to notions of (anti)transitivity, and whether these microscopic patterns give rise to a polarized macroscopic organization into mutually antagonistic clusters. Both problems are studied in Structural Balance Theory (SBT) [4, 18], which originated from Gestalt psychology and the work of Fritz Heider [20]. Heider proposed that positive relations should be transitive (a friend of my friend is my friend) and negative relations antitransitive (an enemy of my enemy is my friend), i.e. valences of relations should agree between positively linked agents and be opposite for negatively linked ones. These considerations were later formalized and generalized in graph-theoretic terms and used to demonstrate that (anti)transitivity of (negative) positive relations is directly linked to the properties of semicycles, and as a result to clustering and polarization. Namely, polarized macrostates clustered in two antagonistic groups require that all semicycles are positive; that is, the products of the signs of their edges are positive (strong balance property; Fig. 1) [4]. Systems clustered into $k \geq 2$ antagonistic groups require that there are no semicycles with exactly one negative edge (weak balance property) [6]. See Methods, Sec. 4.1, for an overview of the main terms and results of SBT. A more detailed discussion can be found in [4, 6].

SBT specifies strict requirements for signed networks to be balanced (partitioned in antagonistic groups), but real-world systems are rarely organized neatly enough to satisfy them completely. This is why a lot of work in SBT is concerned with measures of the degree of balance (DoB), or partial balance [2], which can be seen as indicators of “distance” from the perfectly balanced state. Such measures are typically directly or indirectly related to the relative frequencies of positive and negative semicycles (or semicycles with exactly one negative edge, in the case of weak balance).

Applying SBT in practice is complicated by the fact that enumerating and counting (semi)cycles is computationally expensive, especially for large graphs. This problem can be partially alleviated via novel algorithms and sampling methods [17], but exact solutions will always remain prohibitively expensive due to the nature of the problem. Thus, several approximations have been proposed which can roughly be divided into two families of local and global measures. Local measures attain efficiency by focusing only on cycles of particular, usually short, lengths, such as 3-cycles (triads). They can be fast, but provide only a limited description of the real structure of a network. Thus, we argue that global measures are preferable.

Several global approaches have been proposed. Some ignore the problem of counting cycles entirely, and instead search for partitions minimizing frustration [13] (the number of edges incompatible with SBT assumptions, see Methods, Sec. 4.4), but they suffer from similar computational constraints due to their combinatorial nature. Others leverage spectral properties of signed graphs and are therefore computationally efficient, but measure only strong balance properties and quantify DoB using the smallest eigenvalue of the signed Laplacian matrix [26], which is not normalized and can be difficult to compare between networks. The last major approach is based on approximating cycle counts via counts of closed walks which can be calculated, or at least approximated, very efficiently with standard linear algebra [10, 23, 46]. Moreover, it can produce both local and global measures as well as capture strong and weak balance properties. On the other hand, walk-based approximations can be misleading as they may combine patterns found at very different cycle lengths [17]. It is not immediately clear how such multiscalar information should be aggregated into a single numeric DoB measure. Crucially, most of the existing walk-based ap-

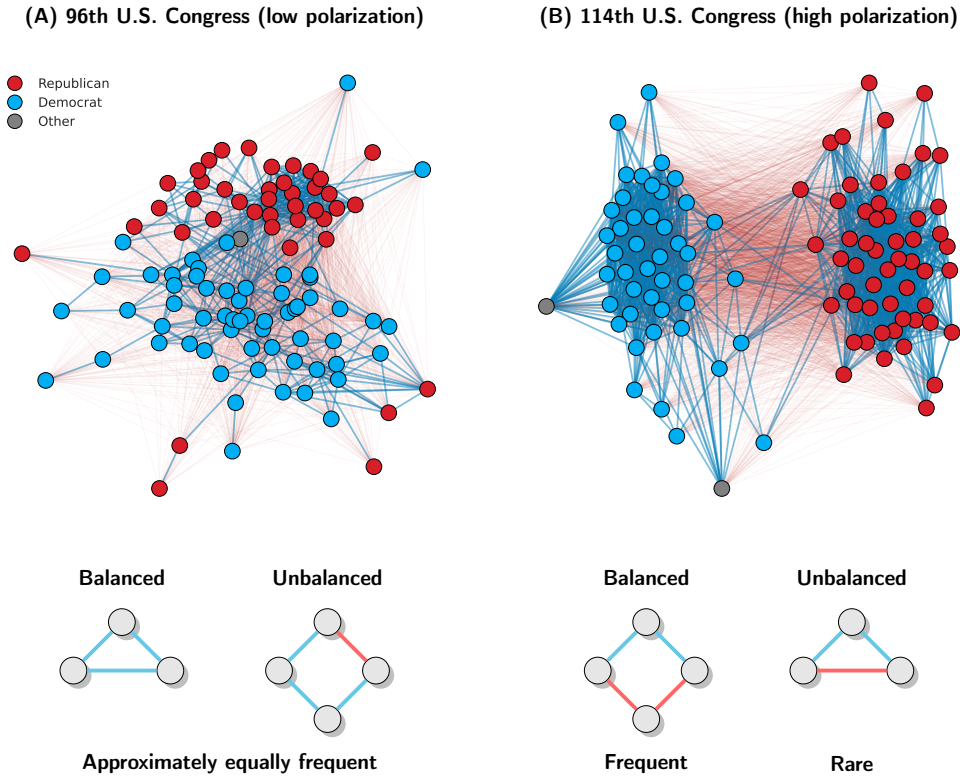


Figure 1. Example of high and low polarization in a social system. Two networks of bill co-sponsorship in the U.S. Senate. Positive ties (blue) link senators, who tended to promote the same bills together more often than by chance, and negative ties (red) correspond to those who collaborated less often than what would be expected by chance. See Sec. 2.3 for the data description and a detailed analysis. **(A)** 96th Congress (1979-81, Carter administration) was a period of low polarization with frequent positive between-party and negative within-party links. This translated to approximately equal frequencies of balanced (positive product of edge signs) and unbalanced (negative product of edge signs) cycles. **(B)** 114th Congress (2015-17, Obama administration) featured high polarization with in-group ties being almost exclusively positive and out-group ties negative. This induced a distribution skewed significantly towards balanced (positive) cycles.

proaches [2, 10, 17, 23, 46] are defined in terms of closed walks which approximate ordinary cycles, while SBT theorems are concerned with semicycles which should be approximated with semiwalks. This is a subtle yet important difference, which may significantly affect results produced by walk-based approximations for directed networks.

Here we propose Multiscale Semiwalk Balance (MSB): an approach applicable to (un)directed, (un)weighted signed networks without self-loops and multilinks. It is multiscale as it provides both local measures approximating DoB at particular cycle lengths and global indicators aggregating local measures across multiple scales in a principled manner. Namely, it accounts for the fact that counts of closed walks grow geometrically, where longer walks typically outnumber shorter very quickly and produce DoB estimates biased towards long-walk patterns. This violates what we call the Locality Principle (LP), which states that short semicycles matter more than long ones. This

was observed already by Cartwright and Harary [4], and later justified empirically by demonstrating that it is easier for people to memorize valences of ties in shorter cycles [55]. More recently, analyses based on counting simple cycles demonstrated that real networks often have a relatively low cycle length threshold after which DoB measures quickly decrease, indicating that structural balance is driven by structures at smaller scales [17].

Our work builds on the Walk Balance (WB) approach proposed by Estrada and Benzi [10], for which it was noticed that it tends to underestimate DoB, especially in large networks [17, 46]. We show that this is caused by too much weight being placed on long cycles and can be fixed by introducing a formal resolution parameter. Namely, we demonstrate how the inverse temperature parameter, β , considered briefly by the authors, can be reinterpreted and used to determine the range of cycle lengths across which DoB measures should be aggregated. It also allows our MSB approach to be applicable and meaningful in the context of weighted signed networks. Additionally, we generalize the WB approach to capture both strong and weak balance, as well as define DoB measures not only at the level of entire graphs but also for particular nodes and pairs of nodes to enable the development of effective SBT-aware clustering methods. Furthermore, by using semiwalk-based approximations our methods are more directly linked to SBT theorems and therefore meaningful for directed signed networks.

We demonstrate the utility of our approach in two case studies of polarization in social systems. The first is a re-analysis of the famous Sampson’s Monks dataset [44], in which we show that the commonly accepted “ground truth” partition is not SBT-optimal by finding a better one, which also sheds some additional light on the underlying social dynamics. In the second study we use our methods to provide strong evidence for increasing polarization in the U.S. Congress based on bill co-sponsorship data [36].

1.1. Notation

Here we consider weighted graphs $G = (V, E, \omega)$ with $|V|$ vertices and $|E|$ edges and no self-loops or multilinks, where V, E are vertex and edge sets respectively, and $\omega : E \rightarrow \mathbb{R}$ is a function assigning weights to edges. The weights can be negative, so the above definition captures all (un)signed, (un)weighted and (un)directed graphs. An unsigned graph induced by an arbitrary graph G will be denoted by $|G| = (V, E, |\omega|)$.

The adjacency matrix of a graph G is given by a square $n \times n$ matrix $\mathbf{A}(G)$ such that $\mathbf{A}_{ij} = \omega(i, j)$ if $(i, j) \in E$ or otherwise $\mathbf{A}_{ij} = 0$. Whenever possible without introducing ambiguity, we will drop the explicit dependence on G and prefer a simpler notation, \mathbf{A} . Matrix trace will be denoted by $\text{tr } \mathbf{A}$ and Hadamard (elementwise) matrix product by \otimes .

2. Results

2.1. Multiscale Semiwalk Balance approach

Here we introduce the Multiscale Semiwalk Balance (MSB) approach to SBT. We first develop it without considering the role of edge weights, which, as discussed below, appear in our approach naturally also in the context of unweighted networks. Once the core framework is established, we show that it automatically extends to weighted graphs in a meaningful way. The main text focuses on strong balance, while the analogous measures of weak balance are discussed in Methods, Sec. 4.3.

2.1.1. Semiwalks and semiadjacency matrix

We start by defining semicycles and semiwalks [54]:

Definition 1 (Semicycle). *A semicycle is a closed walk in which each directed edge can be traversed both ways but only once and each intermediate node is visited exactly once.*

Corollary. *A directed cycle is also a semicycle and a semicycle of length 2 is also a proper cycle.*

Definition 2 (Semiwalk). *A semiwalk is a sequence of edges such that for every two consecutive edges (i, j) and (k, l) it holds that $k \in \{i, j\}$ or $l \in \{i, j\}$.*

Following the main idea behind all walk-based approaches, we will approximate semicycles with closed semiwalks. Note that the above definition implies that semiwalks are equivalent to ordinary walks on an undirected multigraph induced by a directed graph after edge directions are ignored. Fig. 2 shows examples of the connection between cycles and semicycles.

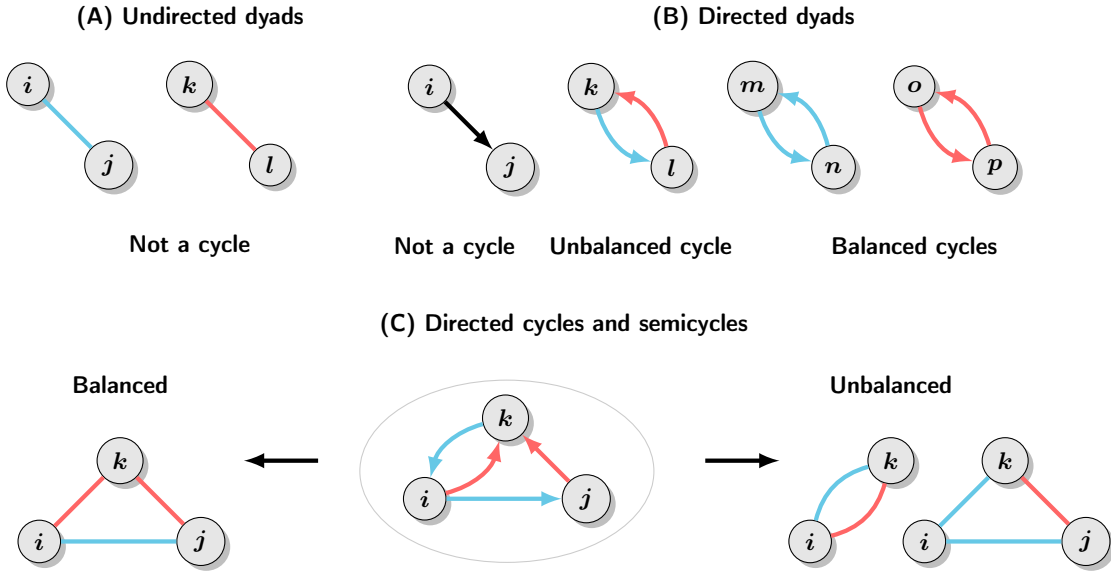


Figure 2. Relationship between signed cycles and semicycles. **(A)** Dyads in undirected networks do not generate any semicycles, as this would imply crossing the same edge twice. Moreover, closed 2-walks in undirected signed networks are always trivially balanced, since $1^2 = (-1)^2 = 1$. **(B)** A single directed edge does not generate any semicycles, as by definition when making a cycle it can be crossed only once. On the other hand, fully-connected dyads generate proper semicycles which are balanced when the relation is symmetric and unbalanced otherwise. **(C)** General relationship between directed cycles and semicycles. Edges in semicycles are treated as if they were bidirectional, so the problem is equivalent to considering cycles in an undirected multigraph in which each pair of nodes may be connected by one or two edges, and each edge can be traversed only once.

To count efficiently, we introduce a semiadjacency matrix operator defined as the symmetric part of an adjacency matrix:

$$\mathbf{S}(G) = \frac{1}{2} (\mathbf{A}(G) + \mathbf{A}(G)^\top) \quad (1)$$

Note that the $1/2$ factor in front ensures that $\mathbf{S}(\mathbf{X}) = \mathbf{X}$ for any symmetric matrix \mathbf{X} . Moreover, $\mathbf{S}(\mathbf{X})$ is symmetric by definition. Thus, the operator is idempotent, that is, $\mathbf{S}(\mathbf{S}(\mathbf{X})) = \mathbf{S}(\mathbf{X})$. Importantly, $\mathbf{S}(G)$ represents an undirected weighted simple graph instead of an undirected unweighted multigraph. Moreover, when G is signed, $\mathbf{S}_{ij} = 0$ whenever $\omega(i, j) = -\omega(j, i)$. However, this is not a problem for counting signed semiwalks because a pair of edges (i, j) and (j, i) with opposite signs would generate the same number of semiwalks with opposite signs, which would eventually cancel each other out during DoB calculations. Moreover, the fact that $\mathbf{S}(G)$ is weighted is also of no consequence, because, as we show later, in our approach all graphs are treated as if they are weighted. Lastly, $\mathbf{S}(G)$ is always symmetric. Thus, by the spectral theorem [38], it is always diagonalizable and has real eigenvalues and eigenvectors.

Semiadjacency matrices can be used to count semiwalks in the same way adjacency matrices can, so \mathbf{S}^k counts semiwalks of length k joining all pairs of nodes. In particular, following Eq. (16) (Methods, 4.2), a matrix with weighted counts of semiwalks of lengths $k_0, k_0 + 1, \dots, k_1 - 1, k_1$ between nodes i and j in an unsigned graph $|G|$ is given by a truncated matrix exponential, $\exp_{k_0}^{k_1} [\beta \mathbf{S}(|G|)]$.

Crucially, SBT is concerned with properties of semicycles, and semiwalks of lengths 0 and 1 cannot be cycles. Moreover, in undirected networks cycles of length 2 are always trivially balanced, so 2-cycles should not be included when measuring structural balance and hence $k_0 = 3$ in this case. On the other hand, \mathbf{S} is symmetric, so it always produces trivially balanced 2-semicycles. Thus, 2-semicycle counts in directed networks should be determined using the raw adjacency matrix, \mathbf{A} , since 2-cycles and 2-semicycles are equivalent. Thus, the weighted count of semiwalks in an (un)directed unsigned graph $|G|$ is given by:

$$\mathbf{W}(|G|, \beta) = \begin{cases} \exp_3^{k_1} [\mathbf{S}(|G|, \beta)], & \text{if } |G| \text{ is undirected} \\ \frac{\beta^2}{2} \mathbf{A}(|G|)^2 + \exp_3^{k_1} [\mathbf{S}(|G|, \beta)], & \text{otherwise} \end{cases} \quad (2)$$

where β is a free parameter used for controlling the amount of weight put on short and long closed semiwalks. In Sec. 2.1.3 we show a principled way for finding an appropriate value of β informed by the Locality Principle.

Furthermore, there are no semicycles longer than the number of nodes, n , so $k_1 \leq n$, and, since higher order terms in the exponential power series die off very quickly, typically $k_1 \ll n$ approximates $k_1 = n$ very well.

2.1.2. Strong balance

Following Estrada and Benzi [10], we note that if $|G|$ is induced by a signed graph G , then elements of \mathbf{W} give weighted counts of balanced (positive) and unbalanced (negative) walks together, $\mathbf{W}(|G|, \beta)_{ij} = \mu_{ij}^+ + \mu_{ij}^-$. For the original signed graph G one gets the difference between weighted counts of balanced and unbalanced walks, $\mathbf{W}(G, \beta)_{ij} = \mu_{ij}^+ - \mu_{ij}^-$.

Counts of closed semiwalks are given by the diagonal elements, so the overall counts are given by appropriate matrix traces. Thus, to measure structural balance in a signed network one can use the Balance Index [10], or the ratio of the difference between weighted counts of balanced and unbalanced walks to the count of all walks irrespective of signs:

$$K_S(G, \beta) = \frac{\mu^+ - \mu^-}{\mu^+ + \mu^-} = \frac{\text{tr } \mathbf{W}(G, \beta)}{\text{tr } \mathbf{W}(|G|, \beta)} \quad (3)$$

A conceptually simpler measure is Degree of Balance (DoB), proposed already by Cartwright and Harary [4], which represents the proportion of balanced walks:

$$B_S(G, \beta) = \frac{\mu^+}{\mu^+ + \mu^-} = \frac{1}{2} [K(G, \beta) + 1] \quad (4)$$

Following [10] again, we can define node-level measures simply by calculating diagonals instead of traces:

$$K_S(G, \beta, i) = \frac{\mathbf{W}(G, \beta)_{ii}}{\mathbf{W}(|G|, \beta)_{ii}} \quad (5)$$

$$B_S(G, \beta, i) = \frac{1}{2} [K_S(G, \beta, i) + 1] \quad (6)$$

Moreover, measures of balance at a particular semicycle length k can also be easily defined:

$$K_S(G, k) = \frac{\text{tr } \mathbf{S}(G)^k}{\text{tr } \mathbf{S}(|G|)^k} \quad (7)$$

$$B_S(G, k) = \frac{1}{2} (K_S(G, k) - 1) \quad (8)$$

Note that this measure does not depend on β , since, even if it did, the same weighting factor would have to appear in both the numerator and denominator. This shows that β indeed controls only the amount of weight put on different cycle lengths, but does not influence the degree of balance at particular lengths.

2.1.3. Contribution profiles and the Locality Principle

Using truncated exponentials defined in Eq. (16), one can assess the contribution of closed semiwalks of length k to the total weighted sum of semiwalk counts for lengths k_0, \dots, k_1 :

$$C(G, \beta, k) = \frac{\beta^k}{k!} \times \frac{\text{tr } \mathbf{S}(|G|)^k}{\text{tr } \mathbf{W}(|G|, \beta)} \quad (9)$$

In other words, Eq. (9) measures the ratio of the weighted sum of closed semiwalks of length k to the total weighted sum of semiwalks over a specified range of lengths. It is normalized by construction, so $C(\dots) \in [0, 1]$ and $\sum_k C(\dots, k) = 1$.

The contribution score clearly depends on β , which can be used for controlling the influence of different length scales on the overall calculations. This is a crucial feature of our approach as it provides a straightforward operationalization of the Locality Principle: shorter cycles should generally matter more than longer cycles. In more technical terms, the contribution score can be used to identify a range of reasonable values for β . Namely, it should be that $\beta \in (0, \beta_{\max}]$, where:

$$\beta_{\max} := \max \beta \quad \text{s.t.} \quad C(G, \beta, k_0) > \dots > C(G, \beta, k_1) \quad (10)$$

Finally, following the parsimony principle, we choose the weakest LP assumption possible and set $\beta = \beta_{\max}$. Thus, β plays the role of a resolution parameter setting the range of cycle lengths across which DoB should be assessed. Moreover, it can be shown that β_{\max} always exists and indeed controls the weights put on closed (semi)walks of different lengths (see sec. S1 of Supplementary Information (SI) for the proof).

Our results also explain why the original WB approach [10] underestimates DoB in large networks. Namely, it does so because without determining the characteristic scale of a network by tuning β , the contribution profile may peak over very long cycles (Fig. 3). Crucially, this problem is likely to affect any other walk-based methods, which do not use a well-tuned resolution parameter. Moreover, without a measure akin to Eq. (9), it is hard to know for sure whether a given method will produce correct results for a given network.

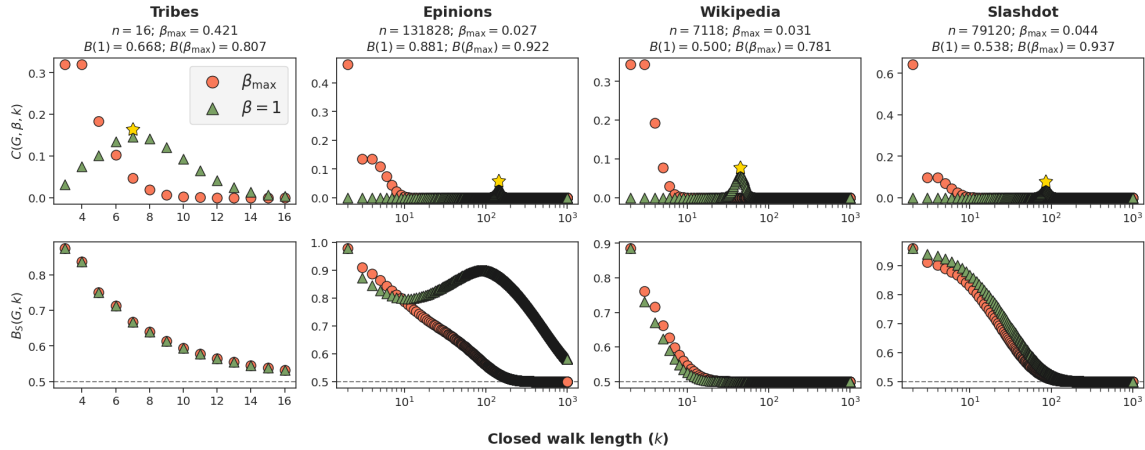


Figure 3. Contribution (top) and local balance (bottom) profiles in four real networks studied by Estrada and Benzi [10] (see Methods, Sec. 4.7, for dataset descriptions) based on WB ($\beta = 1$) and MSB (β_{\max}) approaches. Approximations based on $m = 10$ leading eigenvalues from both ends of the spectrum were used. Evidently, WB places most of the weight on very long cycles ($k \approx 100$) in large networks, which clearly violates LP. As a result, it produces much lower DoB estimates than MSB, since products of signs over very long closed walks are arguably mostly random. Only in the case of Epinions network WB produces an estimate close to the one given by MSB. However, as balance measures at particular cycle lengths show, this happens only because of the very particular structure of the network resulting in high DoB at cycle lengths of approximately 100. Moreover, this seems to be a statistical artifact which disappears almost completely when balance is assessed based on semiwalks (MSB) instead of ordinary walks (WB).

2.1.4. The Locality Principle and psychosocial constraints

The Locality Principle is justified also by a long history of social and psychological research. Indeed, it represents one of the three core principles of social influence theory [27], and has been extensively observed in empirical studies of social networks [31]. Not only has it been well-documented that geographical proximity is an important predictor of social influence [3, 15, 33], but social proximity (friends vs. strangers) has also been shown to be a key factor across numerous areas of research [8, 22, 30].

Recently, [52] analyzed a global dataset and found that close social connections had the strongest effect on people to follow social distancing guidelines amidst the COVID-19 pandemic. Studies of social networks have demonstrated various domains of influence that are affected by social proximity, including attitudes in an online music community [8], online purchasing behavior [30], and information sharing on Twitter [56]. Thus, we argue that the Locality Principle is a central psy-

chosocial factor constraining the flow of information and influence in social networks, and therefore should be accounted for in operationalizations of SBT.

2.1.5. Communicability and β as inverse temperature

We already established that β controls the impact that shorter and longer walks have on assessing structural balance. In line with previous models of network centrality based on statistical physics [11, 24], β can be considered an inverse temperature parameter, which quantifies how much energy a random walker exploring a given network spends, or disperses, while traversing its links and nodes [12, 16]. Here, both WB and MSB are closely related to the notion of communicability [11, 12], which is defined as the exponential of the adjacency matrix rescaled by the inverse temperature, $\exp \beta \mathbf{A}$. Truncation notwithstanding, this definition coincides with our Eq. (2). Given the nature of communicability as the energy spent or the information exchanged by a network of quantum harmonic oscillators to sync, β can be interpreted as the inverse temperature of the system [12]. As the “temperature” approaches infinity, i.e. when $\beta \rightarrow 0$, less and less information flows between nodes and only the shortest scales matter. In fact, one can check that the density matrix ρ — relative to the entanglement of such exchange [16] — scales as $\rho_{\beta \rightarrow 0} \propto \mathbf{I} + \beta \mathbf{A}$, which means that only short-range connections influence information exchange. In the extreme case $\beta = 0$, no information flows between nodes and this (lack of) exchange becomes trivially independent of the network topology. However, there is another limit in which network topology does not influence the exchange of information, but for rather different reasons. When the temperature decreases and $\beta \rightarrow \infty$, the information flow becomes so high as to become independent of the network topology, so in this regime any distinction between shorter and longer scales is lost [12]. In between these two extremes, there is a finite value $\beta = \beta_{\max}$ (see Eq. 10) that describes the characteristic length of a system by determining the maximal correlation range, which is still consistent with the Locality Principle. As a result, LP provides a useful heuristic allowing for treating β as a resolution parameter determining the most appropriate scale, or rather a weighted average of scales or cycle lengths, for evaluating degree of balance. Without this physical interpretation and parameter tuning, (semi)walk-based estimates of DoB may not be meaningful.

2.1.6. Weighted measures and β as average edge weight

β can also be interpreted in terms of an average edge weight. Any unweighted network can be seen as a weighted network with uniform absolute edge weights of 1. Note that in this case the absolute product over a closed semiwalk of any length is always equal to 1, so every semiwalk is considered equal, and it is only β that controls the characteristic length of the system by re-scaling edge weights, which induces nonuniform semiwalk weights (through β^k scaling). Thus, an arguably natural way to handle non-unitary weights is to re-scale them, so the average absolute weight is equal to 1:

$$w'_{ij} = \frac{mw_{ij}}{\sum_{kl} |w_{kl}|} \quad (11)$$

where $m = |E|$ is the number of edges.

This retains the interpretation of β in terms of an average edge weight and ensures that in a network with a completely trivial topology (i.e. Erdős–Rényi random graph with randomly and independently assigned signs and absolute weights) the expected value of a semiwalk weight (i.e. the product of the corresponding edge weights) gets fixed to 1 when $\beta = 1$.

2.1.7. Pairwise measures and clustering

MSB approach can be also used to define pairwise measures of DoB “between” any two nodes i and j . Such a pairwise notion of DoB makes sense because it is directly connected to yet another SBT theorem [4].

Theorem 1 (Strong structure theorem (alternative)). *A signed graph is strongly balanced if and only if all semipaths joining the same pair of nodes have the same sign.*

This view of SBT makes it explicit that structural balance is determined not only by properties of semicycles but also semipaths (from which the semicycles are formed). Thus, it is justified to define pairwise balance measures, which, as it turns out, follow the same logic as before. Namely, strong pairwise Balance Index and DoB can be defined simply as:

$$K_S(G, \beta, i, j) = \frac{\mathbf{W}(G, \beta)_{ij}}{\mathbf{W}(|G|, \beta)_{ij}} \quad (12)$$

$$B_S(G, \beta, i, j) = \frac{1}{2} (K_S(G, \beta, i, j) - 1) \quad (13)$$

Pairwise DoB measures are important because they allow developing SBT-aware clustering methods. We leave a detailed study of this idea for future work. However, in what follows we use pairwise measures together with standard agglomerative hierarchical clustering [19] (see Methods, Sec. 4.5, for details) to show that MSB approach produces meaningful results such as detecting network partitions of objectively higher quality than “ground truth” solutions frequently assumed in the SBT literature.

2.2. Re-analysis of Sampson’s Monastery dataset

Sampson’s Monastery study [44] produced one of the most famous network datasets studied in Social Network Analysis (SNA) in general, and SBT in particular. It describes the evolution of the social structure in a group of postulants and novices in a monastery in New England in 1960’s. Namely, a network of liking (positive) and disliking (negative) relations was measured at five points in time (see Methods, Sec. 4.7.5, for details). The dataset is particularly valuable because, as the study had been conducted, the group went through a major conflict, which eventually lead to either resignation or expulsion of the majority of the members of the congregation. Moreover, Sampson identified a partition into three groups, which later have been independently validated with analytic SBT-motivated clustering methods [9], and therefore is commonly recognized as the “ground truth” solution.

The most important events happened at times $t = 2, 3, 4$, which correspond to a period of differentiation and polarization [9] that eventually lead to an open conflict and disintegration of the group. At $t = 2$ twelve new members joined the monastery, while some older members left after $t = 1$, so the new group consisted of 18 men in total. This perturbation lead to an emergence of two competing groups (Loyal Opposition and Young Turks) as well as a group of peripheral members, who were not fully accepted by the rest (Outcasts). The network at time $t = 4$ depicts the structure just before the open conflict and disintegration. At $t = 5$ only 7 members remained in the monastery, and those who stayed (they are marked with red labels on Fig. 4C, $t = 4$) belonged almost exclusively to the Loyal Opposition, which clearly “won” the conflict.

Here we use MSB approach to demonstrate that the “ground truth” partition is not SBT-optimal, or maximally consistent with Theorem 3. This can be measured objectively in terms of frustration

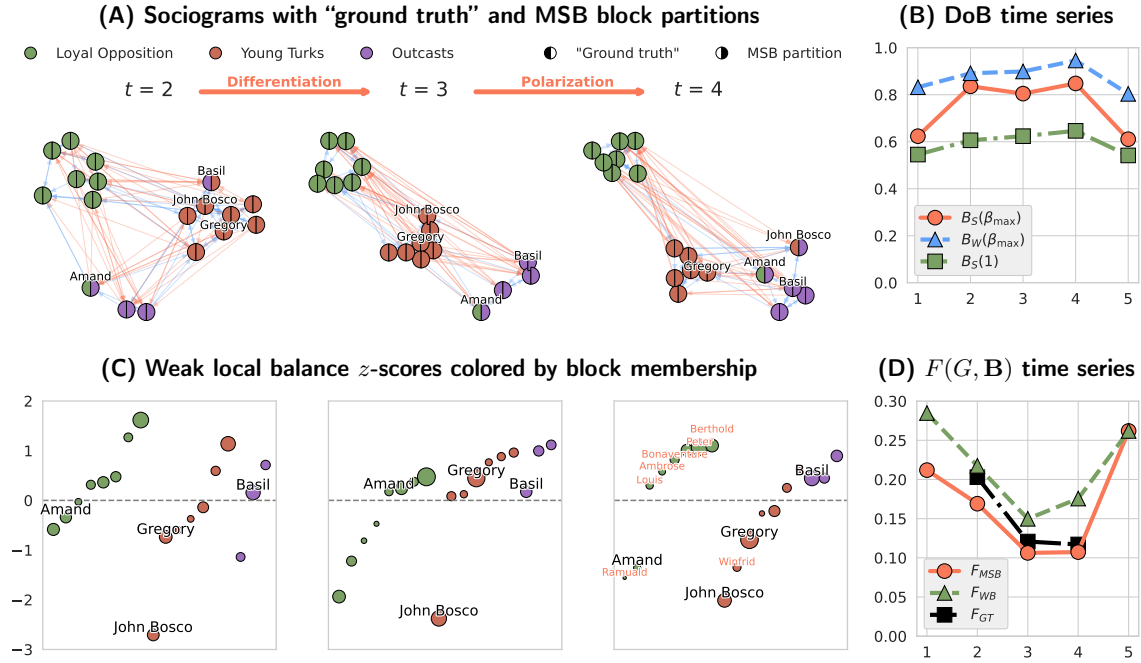


Figure 4. Re-analysis of Sampson’s Monastery networks using SWB approach. Full spectra were used in computations (exact results). **(A)** Signed sociograms at times $t = 2, 3, 4$. Left side colors denote block membership according to the “ground truth” partition and right side colors correspond to SWB partitions. Positive ties are blue and negative are red. Individuals of which “ground truth” and SWB block memberships differ (Amand, Basil and John Bosco) as well as the leaders of Young Turks (John Bosco and Gregory) are labelled. Network layout was determined with Kamada-Kawai algorithm using only positive ties with weights (distances) on cross-block ties rescaled by the factor of 5. **(B)** Time series of strong and weak SWB DoB measures as well as strong DoB based on WB approach of Estrada and Benzi [10], which is equivalent to SWB approach with $\beta = 1$ using ordinary adjacency matrix. **(C)** Weak local balance expressed as z -scores relative to the overall distribution. Points are sized proportionally to local contributions and ordered first by block membership and then by balance scores. Members who remained at the monastery after the culmination of the conflict ($t = 5$) are marked with red labels on the subplot for $t = 4$. **(D)** Time series of frustration indices (see Methods, Sec. 4.4) according to partitions obtained with SWB and WB ($\beta = 1$) approaches as well as the “ground truth” solution (which is defined only for times $t = 2, 3, 4$).

index, $F(G, \mathbf{B})$ (Methods, Sec. 4.4). We show that there is a partition with lower frustration and that it has a meaningful interpretation leading to a deeper understanding of the social dynamics at play.

Fig. 4A shows both the “ground truth” and the MSB network partitions for times $t = 2, 3, 4$ (see Methods, Sec. 4.5). They differ only in a few details, which are, nonetheless, very informative about the unfolding dynamics. Firstly, according to the “ground truth” partition, Basil was a member of the Outcasts. However, MSB analysis indicates that initially ($t = 2$) he interacted mostly with the Young Turks and only later was rejected and became one of the Outcasts. Secondly, Amand, a member of the Loyal Opposition according to the “ground truth”, was consistently identified as

one of the Outcasts by our MSB clustering procedure. Most importantly, according to MSB, John Bosco, who was considered one of the two leaders of the Young Turks (the second one was Gregory), became one of the Outcasts just before the disintegration of the monastery ($t = 4$). This says a lot about why the Young Turks “lost” the competition against the Loyal Opposition, of which core constituted most of the group that remained at the monastery.

As evident in Fig. 4C, local weak balance scores of John Bosco were consistently low and at time $t = 4$ also Gregory, the second leader, attained low local balance. This was largely driven by the tension in their personal relationship (at $t = 4$ the Gregory→John Bosco tie is positive and John Bosco→Gregory is negative), which then propagated through the entire group (note that both of them had high local contribution scores, Fig. 4C) leading, probably, to its decomposition. As Fig 4A shows, over time John Bosco established more positive connections with Outcasts and developed negative feelings towards Gregory. At the same time, the core of Loyal Opposition strengthened internal connections and became very cohesive at time $t = 4$, as indicated by high weak local balance scores of most of the individuals with red labels on Fig. 4.

Last but not least, MSB measures of DoB are clearly high during the evolution of the conflict ($t = 2, 3, 4$), with the maximum at $t = 4$, while analogous WP measures, which are not based on LP, yielded markedly lower DoB values that cannot be readily interpreted as indicative of a conflict, as they are not much greater than $1/2$ (which can be expected for a random assignment of edge signs). Similarly, frustration values obtained with MSB clustering are consistently lower than those of “ground truth” partition, and at times $t = 1, 2, 3, 4$ also lower than the ones obtained using WB.

Thus, the analysis indicates that MSB may be used to produce high quality, meaningful results, which can be even better than popular “ground truth” solutions. Moreover, through a combination of global and local measures an in-depth understanding of the underlying dynamics may be achieved.

2.3. Polarization in the U.S. Congress

It is often claimed that political life in contemporary democracies have polarized significantly over the last few decades. Arguably, this debate is particularly relevant for the U.S., because of its largely two party political system, for which the notion of (bi)polarization is particularly well-defined. Such a hypothesis is also supported by a lot of empirical evidence (cf. [21, 36] and references therein).

Here we use MSB approach to study polarization in both chambers of the U.S. Congress based on patterns of bill co-sponsorship between 1973 and 2016 (93rd to 114th Congress) [36]. The dataset consists of two sequences of signed networks (see Methods, Sec. 4.7.6 for details) inferred from co-sponsorship data, where positive ties indicate statistically significant tendency of two representatives/senators to promote the same bills and negative ties the opposite tendency to not work on the same projects.

Our analysis indicates that polarization increased markedly in both the House of Representatives (Fig. 5A) and the Senate (Fig. 5B). This is evident in the steadily increasing strong DoB values meaning that co-sponsorship networks became easier to bipartition in time. Interestingly, and consistently with our previous analysis of the importance of Locality Principle, WB approach yielded almost exclusively very low DoB values, and thus would not capture the true trend. This is, of course, the consequence of the violation of LP.

In both chambers frustration index values clearly converge (Fig. 5, 2nd panels) meaning that optimal bipartitions and optimal clusterings (in k groups) based on MSB approach, as well as partitions following partisan affiliations are becoming more and more consistent with the SBT theorems and therefore also similar. This is evident in the time series of the similarity between

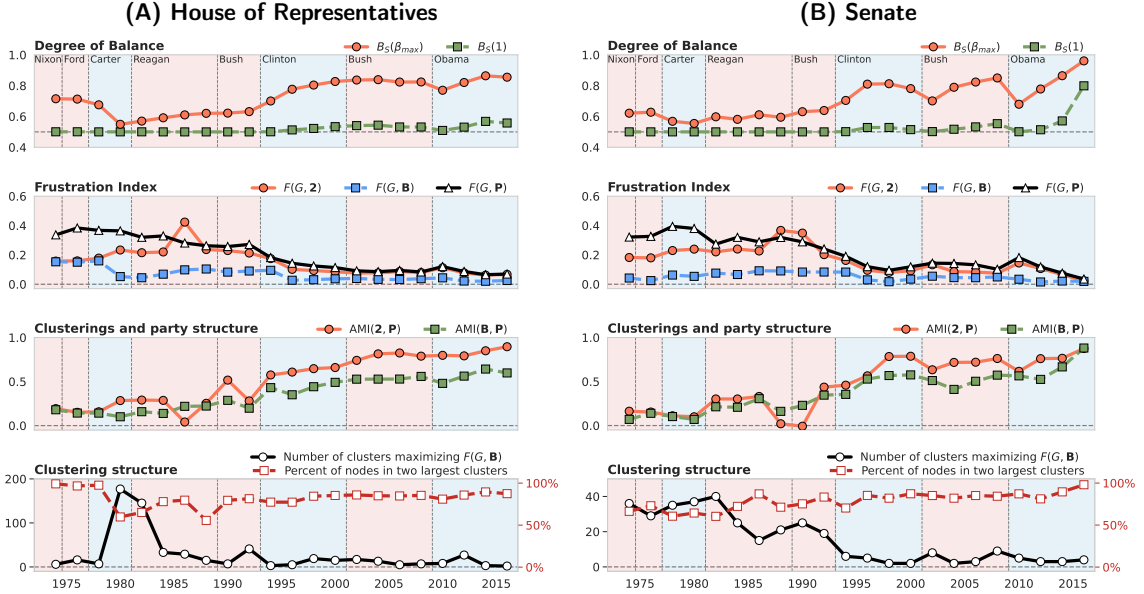


Figure 5. Polarization in the U.S. Congress between 93th and 114th Congress (1973-2016). Panels are divided into regions corresponding to subsequent White House administrations with colors denoting Republican (red) and Democratic (blue) presidents. Approximations based on $m = 10$ leading eigenpairs from the both ends of the spectrum were used. Starting from the top, **(1st panel)** shows strong DoB time series based on MSB approach, $B_S(\beta_{max})$ and WB of Estrada and Benzi [10], $B_S(1)$. **(2nd panel)** presents values of frustration index for optimal partitions into 2 clusters, $F(G, 2)$, general partitions minimizing $F(G, B)$, and partitions based on partisan affiliations, $F(G, P)$. **(3rd panel)** quantifies similarity between party-based partitions and optimal bipartitions, $AMI(2, P)$, as well as optimal partitions into k clusters, $AMI(B, P)$, using Adjusted Mutual Information (AMI) score [53]. The closer values are to 1, the better is the match between two clustering solutions. **(4th panel)** shows the number of clusters in the solution minimizing $F(G, B)$ (left y -axis), as well as the fraction of nodes within the two largest clusters (right y -axis).

MSB and partisan partitions (Fig. 5, 3rd panels). Moreover, even in k -clusterings with k large, most of the nodes tend to belong to the two largest clusters, indicating, again, an increasingly bipolar structure organized along the party lines.

3. Discussion

Polarization is often considered a salient, and perhaps worrying, feature of contemporary societies [1, 21, 36, 45]. It can result in a sharp divergence of popular beliefs or attitudes (ideological polarization) as well as in-group favouritism and out-group hostility (affective polarization) [21]. Crucially, the latter implies clustering of social networks into 2 or more groups with primarily positive in-group and negative out-group ties. This structural aspect of polarization is studied in Structural Balance Theory (SBT), which links it to properties of semicycles in signed networks and provides strict criteria for measuring polarization [4, 6].

Here we introduced Multiscale Semiwalk Balance (MSB) approach for measuring both strong and weak degree of balance (DoB), which is applicable to any kind of (simple) signed networks, including directed and weighted ones. MSB is computationally efficient by approximating semicycles with semiwalks, which can be counted using standard linear algebra. Crucially, it is explicitly multiscale as it provides both local measures, assessing DoB for cycles of particular length, as well as global measures aggregating local information in a principled manner based on the Locality Principle (LP). The resolution of an analysis is controlled by a single inverse temperature parameter, β , which can be tuned based on first principles to capture the characteristic scale of a network at which its DoB should be assessed. This is a crucial feature of our framework, as even though many other approaches apply some decaying weights to longer cycles, typically the decay rate is fixed or controlled by a free parameter with no principled way of selecting an appropriate value [2, 10, 17, 23, 46].

Real networks rarely fully satisfy the requirements of the structure theorems of SBT, so in practice measures of partial balance, or degree of balance, are used [2, 4]. Such measures are often based on comparing relative frequencies of balanced and unbalanced cycles, but it is not immediately clear how cycles of different lengths should be weighted to produce meaningful results. MSB solves this problem by following the Locality Principle (LP), which motivates a principled weighting scheme for aggregating relative counts across different lengths. Our results show that this allows for a very effective analysis of signed networks, including finding clearly interpretable partitions of objectively higher quality (measured with frustration index) than well-known “ground truth” solutions (Sec. 2.2). We also demonstrated that MSB provides useful tools for studying polarization in social systems by providing strong evidence for increasing polarization in both chambers of the U.S. Congress based on bill co-sponsorship data (Sec. 2.3).

LP is justified not only by its usefulness as a heuristic guiding DoB methods, but also by a long history of social and psychological research [8, 22, 27, 30, 31, 55]. This stresses the importance of multiscale approaches to SBT and network science more generally. By linking structural balance to communicability [11, 12], our results suggest that, perhaps, other network descriptors defined in terms of walks, or powers of adjacency matrices, can be informed by Locality Principle. Note that contribution scores defined in Eq. (9), and used for operationalizing LP, can be calculated for any, also unsigned, network. Thus, LP is a heuristic for determining communicability, or the characteristic intensity and length of internode correlations, of a network, and this determines the appropriate weighting scheme for aggregating walk-based measures across multiple length scales. More generally, our results contribute also to research on the importance of local structures in networks [32, 34, 49].

Unlike many other approaches to SBT [10, 23, 46], MSB is formulated explicitly in terms of semicycles and semiwalks. This connects it more directly to the structure theorems [4, 6], and as a result facilitates meaningful analyses of directed networks. Moreover, by linking structural balance to communicability [11] and LP, we proposed a principled interpretation of edge weights in signed networks. Thus, our work may be used to significantly extend the range of applicability of SBT, facilitating research on structural balance and polarization in a wide variety of systems, irrespective of whether they are (un)directed or (un)weighted.

Our methods, of course, are not defined for multilayer or higher-order networks [37]. This stems from the fact that it is not yet entirely clear how to generalize SBT to such systems in a way that would retain the core features of the theory, e.g. reproduce the structure theorems (although some promising attempts have been made [39]). Moreover, in both case studies we analyzed dynamics, or evolution, of social structure. As long as one can assume that the structure does not change significantly on short time scales, it is reasonable to analyze “snapshot” networks aggregating rela-

tions over longer time intervals. This is exactly what we did. Nonetheless, generalizations of SBT to other dynamical frameworks, such as relational event model [48] or stream graphs [5], remains an interesting problem.

Secondly, our approach attains computational efficiency by approximating semicycles with semi-walks, a strategy which can sometimes produce less accurate results than exact (but much less efficient) methods based on counting proper cycles [17]. However, thanks to LP our measures are driven primarily by patterns found in relatively short closed walks, which by definition are more similar to cycles than long walks (closed walks of lengths 2 and 3 are equivalent to 2- and 3-cycles). Moreover, the accuracy of our approach could be improved by reformulating it using non-backtracking (Hashimoto) matrices [51], which would further decrease the discrepancy between closed walks and cycles. Such an extension may be a promising direction for future work.

4. Methods

4.1. Structural Balance Theory

Here we review the main assumptions and results of SBT.

Let iRj denote a relation between entities i and j and $i\neg Rj$ its opposite. Positive and negative relations will be denoted by iLj and $i\neg Lj$ respectively. Now, the assumption of SBT is that relations should be symmetric ($iRj \wedge jR'i \Rightarrow R = R'$), and that positively linked nodes should agree with respect to valences of their other ties ($iLj \wedge iRk \wedge jR'k \Rightarrow R = R'$), while negatively linked should disagree ($i\neg Lj \wedge iRk \wedge jR'k \Rightarrow R = \neg R'$). Moreover, this consistency property should extend to indirect preferences implied by (anti)transitivity over longer chains (e.g. $iLj \wedge j\neg Lk \wedge kRm \wedge iR'm \Rightarrow R' = \neg R$). It is also assumed that such balanced relations are easier/cheaper to maintain and therefore should be more stable in time and generally more frequent than unbalanced ties [4, 20].

The core results of SBT, due to Cartwright and Harary [4], translate the above requirements to specific properties of signed graphs allowing for measurement and practical applications of the notion of structural balance. Below we rehash these results.

Definition 3 (Strong balance property). *A signed graph is balanced if and only if every semicycle it contains is positive (the product over all edge signs is positive).*

Theorem 2 (Strong structure theorem). *A signed graph is balanced if and only if its vertices can be partitioned into two subsets such that positive edges are contained within the subsets and negative ones go between them.*

The above results concerned with 2-clusterability were later generalized by Davis [6], who provided necessary and sufficient conditions for k -clusterability (where $k \geq 2$ is an unknown integer).

Definition 4 (Weak balance property). *A signed graph is k -balanced if and only if no semicycle contains exactly one negative edge.*

Theorem 3 (Weak structure theorem). *A signed graph is k -balanced if and only if its vertices can be partitioned into k subsets such that positive edges are contained within the subsets and negative ones go between them.*

4.2. Analytic functions of real symmetric matrices

Let $\mathbf{X} \in \mathbb{R}^{n \times n}$ be a real symmetric matrix and $f : \mathbb{R}^{n \times n} \rightarrow \mathbb{R}^{n \times n}$ an analytic function defined over the field of real square matrices. Then, $f(\mathbf{X}) = \mathbf{Q}f(\mathbf{\Lambda})\mathbf{Q}^\top$, where $\mathbf{\Lambda}$ is a real diagonal matrix with eigenvalues of \mathbf{X} ($\lambda_1 \geq \lambda_2 \geq \dots \geq \lambda_n$) and the columns of \mathbf{Q} are the corresponding eigenvectors. This implies that:

$$f(\mathbf{X})_{ij} = \sum_{r=1}^n \mathbf{Q}_{ir} f(\lambda_r) \mathbf{Q}_{jr} \quad (14)$$

$$\text{tr } f(\mathbf{X}) = \sum_{r=1}^n f(\lambda_r) \quad (15)$$

In particular, we will be interested in matrix exponentials and finite truncations of their power series:

$$\exp_{k_0}^{k_1}(\beta \mathbf{X}) = \mathbf{Q} \left(\sum_{k=k_0}^{k_1} \frac{\beta^k}{k!} \mathbf{\Lambda}^k \right) \mathbf{Q}^\top \xrightarrow[k_0 \rightarrow 0]{k_1 \rightarrow \infty} \exp(\beta \mathbf{X}) \quad (16)$$

where β is a free parameter that can be used for controlling the rate of growth/decay of the weights attached to different powers of \mathbf{X} , and for $\beta = 1$ the standard exponential is recovered.

4.3. Weak balance

Following Ref. [23] we define non-negative matrices \mathbf{P} and \mathbf{N} corresponding to positive and negative parts of a signed semijacency matrix such that:

$$\mathbf{S} = \mathbf{P} - \mathbf{N} \quad (17)$$

Weak balance is defined in terms of the extent to which a network is free of semicycles with exactly one negative edge. This single negative link can be placed anywhere along a semipath starting at node i . Hence, we first define a matrix counting weakly unbalanced semiwalks of length k between nodes i and j in a signed graph G as:

$$\begin{aligned} \mathbf{V}_k(G) &= \sum_{l=1}^k \mathbf{P}^{l-1} \mathbf{N} \mathbf{P}^{k-l} \\ &= \sum_{l=1}^k \mathbf{Q} \mathbf{\Lambda}^{l-1} \mathbf{Q}^\top \mathbf{N} \mathbf{Q} \mathbf{\Lambda}^{k-l} \mathbf{Q}^\top \\ &= \mathbf{Q} \left[\left(\sum_{l=1}^k \mathbf{L}(k, l) \right) \otimes \mathbf{M} \right] \mathbf{Q}^\top \end{aligned} \quad (18)$$

where $\mathbf{Q} \mathbf{\Lambda} \mathbf{Q}^\top$ is the eigendecomposition of \mathbf{P} , $\mathbf{M} = \mathbf{Q}^\top \mathbf{N} \mathbf{Q}$ and $\mathbf{L}(k, l)_{ij} = \lambda_i^{l-1} \lambda_j^{k-l}$. Moreover, we used the fact that $\mathbf{\Lambda}^{l-1} \mathbf{M} \mathbf{\Lambda}^{k-l} = \mathbf{L}(k, l) \otimes \mathbf{M}$.

Now, a matrix with weighted sums of counts of semiwalks of lengths k_0, \dots, k_1 joining nodes i and j is given by:

$$\mathbf{V}_{k_0}^{k_1}(G, \beta) = \sum_{k=k_0}^{k_1} \frac{\beta^k}{k!} \mathbf{V}_k(G) = \mathbf{Q} \mathbf{U}_{k_0}^{k_1}(G, \beta) \mathbf{Q}^\top \quad (19)$$

$$\mathbf{U}_{k_0}^{k_1}(G, \beta) = \left[\sum_{k=k_0}^{k_1} \frac{\beta^k}{k!} \sum_{l=1}^k \mathbf{L}(k, l) \right] \otimes \mathbf{M} \quad (20)$$

Clearly, once \mathbf{M} is known, $\mathbf{U}_{k_0}^{k_1}(G, \beta)$ can be computed roughly in $\mathcal{O}(k_1^2 m^2)$ time, where m is the number of eigenvalues.

Next, we can use Eq. (19) to calculate the overall weighted sums of counts of unbalanced closed semiwalks from appropriate traces:

$$\text{tr } \mathbf{V}_{k_0}^{k_1}(G, \beta) = \sum_{k=k_0}^{k_1} \frac{\beta^k}{k!} \text{tr } \mathbf{V}_k(G) \quad (21)$$

$$\text{tr } \mathbf{V}_k(G) = k \sum_{i=1}^m \lambda_i^{k-1} \mathbf{M}_{ii} \quad (22)$$

where we used the fact that trace is invariant under cyclic permutations and \mathbf{Q} is orthonormal. The weighted sum of counts of closed semiwalks at a node i is similarly given by the diagonal elements $\mathbf{V}_{k_0}^{k_1}(G, \beta)_{ii}$.

Now, Eqs. (2) and (21) can be used to define the measure of the overall weak balance:

$$B_W(G, \beta) = 1 - \frac{\mu_W}{\mu_B + \mu_U} = 1 - \frac{\text{tr } \mathbf{V}_{k_0}^{k_1}(G, \beta)}{\text{tr } \mathbf{W}(|G|, \beta)} \quad (23)$$

with the local node-level DoB following the same pattern, but using node-specific counts of closed semiwalks. Moreover, weak DoB at a particular length k is given by:

$$B_W(G, k) = 1 - \frac{\text{tr } \mathbf{V}_k(G)}{\text{tr } |\mathbf{S}|^k} \quad (24)$$

Similarly, following the arguments presented in Sec. 2.1.7, weak pairwise DoB is defined as:

$$B_W(G, \beta, i, j) = 1 - \frac{\mathbf{V}_{k_0}^{k_1}(G, \beta)_{ij}}{\mathbf{W}(|G|, \beta)_{ij}} \quad (25)$$

This weak notion of pairwise balance is based on the fact that two nodes are jointly weakly balanced if and only if it holds that if they are connected by a path with only positive edges, then there is no path with exactly one negative edge connecting them. This leads to an analogous alternative weak structure theorem, which justifies the notion of weak pairwise DoB (see SI, Sec. S2, for the proof).

Theorem 4 (Weak structure theorem (alternative)). *A signed graph is weakly balanced if and only if for any pair of nodes it holds that if there is an all positive path between them then there are no paths with exactly one negative edge joining them.*

Last but not least, the matrix series defined in Eq. (19) used for counting unbalanced closed (semi)walks always converges, so it is well-defined. Note that:

$$0 \leq \sum_{k=k_0}^{k_1} \frac{\beta^k}{k!} \sum_{l=1}^k \text{tr} \mathbf{P}^{l-1} \mathbf{N} \mathbf{P}^{k-l} \leq \sum_{k=0}^{\infty} \frac{\beta^k}{k!} \text{tr} (\mathbf{P} + \mathbf{N})^k = \text{tr} \exp(\beta|\mathbf{S}|) \quad (26)$$

where it is known that the rightmost matrix exponential and its trace always converge, so the middle part of the inequality must converge too.

4.4. Frustration index

Very conveniently, SBT provides an objective measure of the quality of a network clustering solution. Since perfect balance implies that negative edges go only between clusters and positive ones are contained within them, a natural clustering quality measure is Frustration Index, which, following Ref. [9], can be defined in terms of the relative weighted count of edges inconsistent with the SBT hypothesis:

$$F(G, \mathbf{B}) = \frac{\mathbf{1}^\top \left[(\mathbf{B}\mathbf{B}^\top) \otimes \mathbf{N} + (\mathbf{1}\mathbf{1}^\top - \mathbf{B}\mathbf{B}^\top) \otimes \mathbf{P} \right] \mathbf{1}}{\mathbf{1}^\top |\mathbf{S}| \mathbf{1}} \quad (27)$$

where $\mathbf{1}$ is a vector of ones of an appropriate length and $\mathbf{B} \in \mathbb{R}^{n \times b}$ is a block-partition matrix such that $\mathbf{B}_{ij} = 1$ if node i belongs to the block j and is 0 otherwise.

4.5. Hierarchical clustering with pairwise DoB measures

Here we will use the following naive yet effective clustering procedure for signed networks based on pairwise DoB measures (see Secs. 2.1.7 and 4.3). Let $\mathbf{D}_{ij}^S = 1 - B_S(G, \beta_{\max}, i, j)$ and $\mathbf{D}_{ij}^W = 1 - B_W(G, \beta_{\max}, i, j)$ be pairwise dissimilarity matrices based on the notions of strong and weak balance respectively and let N_b be the maximum number of clusters one is willing to consider. Then, for $b = 2, \dots, N_b$:

1. Run Hierarchical Clustering (HC) [19] algorithm for b clusters using \mathbf{D}^S as input and calculate frustration index according to Eq. (27) for the obtained block-partition matrix \mathbf{B} .
2. Run HC for b clusters using \mathbf{D}^W as input and calculate the corresponding frustration index.
3. Store the lower of the two frustration indices and its corresponding block partition.

Finally, choose the partition with the lowest frustration index.

4.6. Accuracy, efficiency and numerical stability

All computations of SWB can be implemented in a computationally efficient and accurate manner using approximations based on m leading eigenvalues and eigenvectors from both ends of the spectrum. Leading eigenpairs can be found very efficiently using modern linear algebra routines such as implicitly restarted Arnoldi method [28, 47]. Moreover, numerical stability can be guaranteed by conducting all computations in the log-space and using log-sum-exp trick (to avoid overflow when counting closed walks). This requires a bit of extra care as some eigenvalues may be non-positive. However, zero eigenvalues can be ignored altogether and the calculations can be done over the field

of complex numbers, where the logarithm of any number with non-zero modulus is well-defined, and cast back to real values only at the very end. As a result, SWB methods can be remarkably efficient, even when applied to large systems. Sec. S3 in SI presents an empirical analysis of the efficiency of our implementation using three large real-world networks.

A more in-depth discussion of implementation details is beyond the scope of this paper, but we invite the interested reader to study our source code (see: Data and code availability).

4.6.1. Accuracy of SWB approximations

SWB approach is based on three different approximations. First, it approximates semicycles with closed semiwalks. This is a fundamental design decision ensuring high computational efficiency, but it comes at a price of introducing an error, of which impact is hard to assess. A proper analysis of this problem would require a detailed comparison with methods based on counting proper cycles, such as [17], which is beyond the scope of this paper. However, there are good reasons to believe that the error does not distort the results in a significant way. This is indicated by the high quality and meaningfulness of the empirical results discussed in Secs. 2.2 and 2.3. Moreover, by satisfying the Locality Principle, SWB ensures that DoB measures are driven primarily by patterns found in short closed walks, which coincide with cycles much more often than long walks.

The second approximation happens when truncating power series to include only the terms of orders k_0, \dots, k_1 . However, this approximation introduces no significant error by design, as LP ensures that higher order terms have very low and monotonically decreasing contributions to the overall DoB calculations. Thus, as long as enough terms are included, and typically about a dozen is enough, the truncation introduces no noticeable error. In principle, the lowest number of terms necessary for attaining a given cumulative contribution score can be determined easily by inspecting the contribution profile. However, here we used a simple rule-of-thumb and in all cases, unless specified otherwise, used $k_1 = 30$, which is typically more than enough (see Fig. 6A).

The last approximation happens when only m leading eigenpairs from the both ends of the spectrum are used. This allows for solving the corresponding eigenproblems and running other downstream calculations much faster. Moreover, it is clear from Eqs. (14) and (15) that, as long as $|f(x)|$ is decreasing for $x < 0$ and increasing for $x > 0$, the true value can be accurately approximated using leading eigenvalues/eigenvectors from both ends of the spectrum, especially when the distribution of eigenvalues is highly heterogeneous, that is, the cumulative absolute sum is dominated by just a few leading eigenvalues. Fig. 6B provides an empirical support for this claim.

4.7. Network datasets

4.7.1. New Guinea Highlands tribes

An undirected unweighted signed network of friendships among tribes of Gahuku-Gama alliance structure of the Eastern Central Highlands region in New Guinea [40]. Edge sign indicates either friendship or enmity. Accessed from: https://networks.skewed.de/net/new_guinea_tribes

4.7.2. Epinions trust network

This is a who-trust-whom online social network (directed, unweighted and signed) of a general consumer review site Epinions.com. Members of the site can decide whether to “trust” each other. All the trust relationships interact and form the Web of Trust which is then combined with

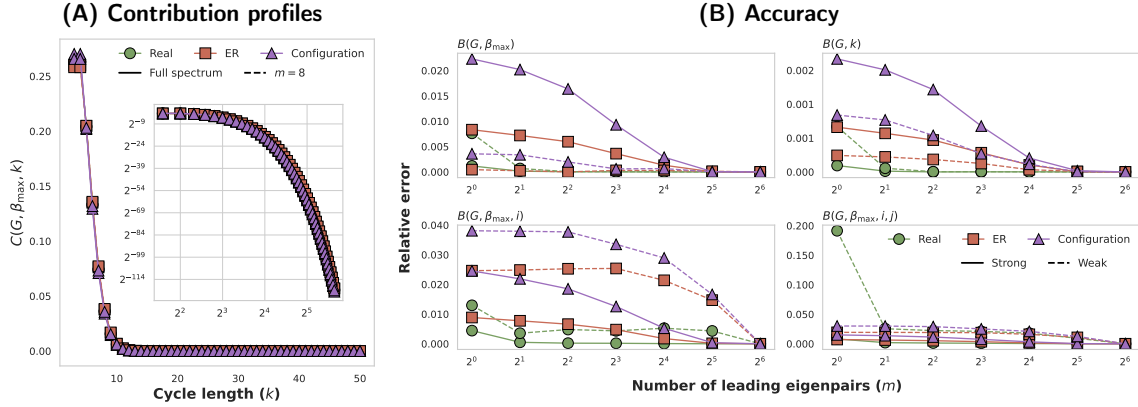


Figure 6. Effects of SWB approximations assessed using bill co-sponsorship network from the U.S. Senate during 114th Congress ($|V| = 100$, $|E| = 3696$) as well as its randomized counterparts based on Erdős–Rényi model and configuration model [37]. **(A)** Contribution profiles are clearly almost identical for the original and randomized networks. Crucially, at $\beta = \beta_{\max}$ almost all the cumulative contribution score is driven by leading low order terms, meaning that higher order terms (roughly $k > 10$) can be safely omitted. **(B)** Errors of DoB measures based on leading eigenvalues calculated relative to values obtained using full spectra. Errors are typically low even for $m = 1$ and in all cases quickly decrease as m increases. Moreover, in most of the cases they are lower for the real network, which is consistent with the fact that errors should be lower for networks with heterogeneous distributions of eigenvalues.

review ratings to determine which reviews are shown to the user [41]. Accessed from: <https://snap.stanford.edu/data/soc-Epinions1.html>.

4.7.3. Wikipedia adminship vote

A directed unweighted signed network of votes on Request for Adminship (RfA) elections from a 2008 snapshot of Wikipedia [29]. Nodes represent editors, and a directed edge (i, j) indicates that editor i voted on editor j . Edge sign indicates the direction of the vote: positive = for, and negative = against. Edges are timestamped. Accessed from: <https://networks.skewed.de/net/elec>.

4.7.4. Slashdot Zoo network

A directed unweighted signed network of interactions among users on Slashdot (slashdot.org), a technology news website [25]. Users name each other as friends (positive tie) or foe (negative tie). The friend label increases the scores of post, and the foe label decreases the score. Accessed from: https://networks.skewed.de/net/slashdot_zoo.

4.7.5. Sampson’s Monastery dataset

Time series of 5 signed directed weighted networks measuring positive and negative relations between postulants and novices in a New England monastery in 1960’s [44]. We used a version of the dataset studied in Ref. [9] in which edges have weights between -3 and 3 correspond-

ing to the ranking of the least and most (dis)liked/(dis)esteemed colleagues. Accessed from: <http://vlado.fmf.uni-lj.si/pub/networks/data/esna/sampson.htm>.

4.7.6. Co-sponsorship relations in the U.S. Congress

Series of directed unweighted signed networks inferred from the data on bill co-sponsorships in both chambers of the U.S. Congress (House of Representatives and Senate) using Stochastic Degree Sequence Model [35, 36]. The data covers the period from 1973 (93rd Congress) to 2016 (114th Congress). Edges are signed, indicating the presence of a significant tendency to co-sponsor, or tendency to not co-sponsor, bills. See SI, Sec. S4, for a table with descriptive statistics. Accessed from: https://figshare.com/articles/dataset/A_Sign_of_the_Times/8096429.

Data and code availability

Sources of the data used in the paper are described in Methods. The code and instructions for replicating the analyses, including a packaged Python code implementing all SWB methods in a user-friendly manner, is available at Github (<https://github.com/sztal/swb>). The repository provides also the datasets used in the analyses.

Acknowledgments

S.T. acknowledges the support of National Science Center, Poland, under a grant number 2020/37/N/HS6/00796 (*Outline of a network-geometric theory of social structure*). A.S.T. acknowledges support from FCT and the LASIGE Research Unit, ref. UIDB/00408/2020 and ref. UIDP/00408/2020.

Author contributions

S.T., M.S., T.J.S. and A.S.T. conceptualized the project. S.T. developed the mathematical framework and its software implementation and conducted the analyses. S.T. and M.S. developed the physical interpretation of the β parameter. S.T. and T.J.S. researched psychological and sociological justification for the Locality Principle. S.T., M.S., T.S. and A.S.T. wrote and reviewed the manuscript.

Competing interests

The authors declare no competing interests.

References

- [1] Samin Aref and Zachary Neal. 2020. Detecting Coalitions by Optimally Partitioning Signed Networks of Political Collaboration. *Scientific Reports* 10, 1 (Jan. 2020), 1506. <https://doi.org/10.1038/s41598-020-58471-z>

- [2] Samin Aref and Mark C Wilson. 2018. Measuring Partial Balance in Signed Networks. *Journal of Complex Networks* 6, 4 (Aug. 2018), 566–595. <https://doi.org/10.1093/comnet/cnx044>
- [3] David R Bell and Sangyoung Song. 2007. Neighborhood effects and trial on the Internet: Evidence from online grocery retailing. *Quantitative Marketing and Economics* 5 (2007), 361–400.
- [4] Dorwin Cartwright and Frank Harary. 1956. Structural Balance: A Generalization of Heider’s Theory. *Psychological Review* 63, 5 (1956), 277–293. <https://doi.org/10.1037/h0046049>
- [5] Salvatore Citraro, Letizia Milli, Rémy Cazabet, and Giulio Rossetti. 2022. Δ -Conformity: multi-scale node assortativity in feature-rich stream graphs. *International Journal of Data Science and Analytics* (2022), 1–12.
- [6] James A. Davis. 1967. Clustering and Structural Balance in Graphs. *Human Relations* 20, 2 (May 1967), 181–187. <https://doi.org/10.1177/001872676702000206>
- [7] Wouter de Nooy. 1999. A Literary Playground: Literary Criticism and Balance Theory. *Poetics* 26, 5-6 (Aug. 1999), 385–404. [https://doi.org/10.1016/S0304-422X\(99\)00009-1](https://doi.org/10.1016/S0304-422X(99)00009-1)
- [8] Sanjeev Dewan, Yi-Jen Ho, and Jui Ramaprasad. 2017. Popularity or proximity: Characterizing the nature of social influence in an online music community. *Information Systems Research* 28, 1 (2017), 117–136.
- [9] Patrick Doreian and Andrej Mrvar. 1996. A Partitioning Approach to Structural Balance. *Social Networks* 18, 2 (April 1996), 149–168. [https://doi.org/10.1016/0378-8733\(95\)00259-6](https://doi.org/10.1016/0378-8733(95)00259-6)
- [10] Ernesto Estrada and Michele Benzi. 2014. Walk-Based Measure of Balance in Signed Networks: Detecting Lack of Balance in Social Networks. *Physical Review E* 90, 4 (Oct. 2014), 042802. <https://doi.org/10.1103/PhysRevE.90.042802>
- [11] Ernesto Estrada and Naomichi Hatano. 2008. Communicability in Complex Networks. *Physical Review E* 77, 3 (March 2008), 036111. <https://doi.org/10.1103/PhysRevE.77.036111>
- [12] Ernesto Estrada, Naomichi Hatano, and Michele Benzi. 2012. The Physics of Communicability in Complex Networks. *Physics Reports* 514, 3 (May 2012), 89–119. <https://doi.org/10.1016/j.physrep.2012.01.006>
- [13] G. Facchetti, G. Iacono, and C. Altafini. 2011. Computing Global Structural Balance in Large-Scale Signed Social Networks. *Proceedings of the National Academy of Sciences* 108, 52 (Dec. 2011), 20953–20958. <https://doi.org/10.1073/pnas.1109521108>
- [14] Eva Ferreira, Susan Orbe, Jone Ascorbebeitia, Brais Álvarez Pereira, and Ernesto Estrada. 2021. Loss of Structural Balance in Stock Markets. *Scientific Reports* 11, 1 (June 2021), 12230. <https://doi.org/10.1038/s41598-021-91266-4>
- [15] Leon Festinger, Stanley Schachter, and Kurt Back. 1950. *Social Pressures in Informal Groups; a Study of Human Factors in Housing*. Harper.

- [16] Arsham Ghavasieh, Massimo Stella, Jacob Biamonte, and Manlio De Domenico. 2021. Unraveling the effects of multiscale network entanglement on empirical systems. *Communications Physics* 4, 1 (2021), 129.
- [17] Pierre-Louis Giscard, Paul Rochet, and Richard C. Wilson. 2017. Evaluating Balance on Social Networks from Their Simple Cycles. *Journal of Complex Networks* 5, 5 (May 2017), 750–775. <https://doi.org/10.1093/comnet/cnx005>
- [18] Frank Harary, Robert Zane Norman, and Dorwin Cartwright. 1965. *Structural Models: An Introduction to the Theory of Directed Graphs*. Wiley.
- [19] Trevor Hastie, Robert Tibshirani, and Jerome Friedman. 2008. *The Elements of Statistical Learning* (second ed.). Springer.
- [20] Fritz Heider. 1946. Attitudes and Cognitive Organization. *The Journal of psychology* 21, 1 (1946), 107–112.
- [21] Marilena Hohmann, Karel Devriendt, and Michele Coscia. 2023. Quantifying Ideological Polarization on a Network Using Generalized Euclidean Distance. *Science Advances* 9, 9 (March 2023), eabq2044. <https://doi.org/10.1126/sciadv.abq2044>
- [22] Herminia Ibarra and Steven B Andrews. 1993. Power, social influence, and sense making: Effects of network centrality and proximity on employee perceptions. *Administrative science quarterly* (1993), 277–303.
- [23] Alec Kirkley, George T. Cantwell, and M. E. J. Newman. 2019. Balance in Signed Networks. *Physical Review E* 99, 1 (Jan. 2019), 012320. <https://doi.org/10.1103/PhysRevE.99.012320>
- [24] Ismo T. Koponen, Elina Palmgren, and Esko Keski-Vakkuri. 2021. Characterising Heavy-Tailed Networks Using q-Generalised Entropy and q-Adjacency Kernels. *Physica A: Statistical Mechanics and its Applications* 566 (March 2021), 125666. <https://doi.org/10.1016/j.physa.2020.125666>
- [25] Jérôme Kunegis, Andreas Lommatzsch, and Christian Bauckhage. 2009. The Slashdot Zoo: Mining a Social Network with Negative Edges. In *Proceedings of the 18th International Conference on World Wide Web - WWW '09*. ACM Press, Madrid, Spain, 741. <https://doi.org/10.1145/1526709.1526809>
- [26] Jérôme Kunegis, Stephan Schmidt, Andreas Lommatzsch, Jürgen Lerner, Ernesto W. De Luca, and Sahin Albayrak. 2010. Spectral Analysis of Signed Graphs for Clustering, Prediction and Visualization. In *Proceedings of the 2010 SIAM International Conference on Data Mining*. Society for Industrial and Applied Mathematics, 559–570. <https://doi.org/10.1137/1.9781611972801.49>
- [27] Bibb Latané. 1981. The psychology of social impact. *American Psychologist* 36, 4 (1981), 343.
- [28] Richard B. Lehoucq, Danny C. Sorensen, and Chao Yang. 1998. *ARPACK Users' Guide: Solution of Large-Scale Eigenvalue Problems with Implicitly Restarted Arnoldi Methods*. SIAM.

- [29] Jure Leskovec, Daniel Huttenlocher, and Jon Kleinberg. 2010. Governance in Social Media: A Case Study of the Wikipedia Promotion Process. *Proceedings of the International AAAI Conference on Web and Social Media* 4, 1 (May 2010), 98–105. <https://doi.org/10.1609/icwsm.v4i1.14013>
- [30] Liye Ma, Ramayya Krishnan, and Alan L Montgomery. 2015. Latent homophily or social influence? An empirical analysis of purchase within a social network. *Management Science* 61, 2 (2015), 454–473.
- [31] Peter V Marsden and Noah E Friedkin. 1993. Network studies of social influence. *Sociological Methods & Research* 22, 1 (1993), 127–151.
- [32] Carolina E. S. Mattsson, Frank W. Takes, Eelke M. Heemskerk, Cees Diks, Gert Buiten, Albert Faber, and Peter M. A. Sloot. 2021. Functional Structure in Production Networks. *Frontiers in Big Data* 4 (May 2021), 666712. <https://doi.org/10.3389/fdata.2021.666712>
- [33] Jannik Meyners, Christian Barrot, Jan U Becker, and Jacob Goldenberg. 2017. The role of mere closeness: How geographic proximity affects social influence. *Journal of Marketing* 81, 5 (2017), 49–66.
- [34] R. Milo, S. Shen-Orr, S. Itzkovitz, N. Kashtan, D. Chklovskii, and Uri Alon. 2002. Network Motifs: Simple Building Blocks of Complex Networks. *Science* 298, 5594 (Oct. 2002), 824–827. <https://doi.org/10.1126/science.298.5594.824>
- [35] Zachary Neal. 2014. The Backbone of Bipartite Projections: Inferring Relationships from Co-Authorship, Co-Sponsorship, Co-Attendance and Other Co-Behaviors. *Social Networks* 39 (Oct. 2014), 84–97. <https://doi.org/10.1016/j.socnet.2014.06.001>
- [36] Zachary P. Neal. 2020. A Sign of the Times? Weak and Strong Polarization in the U.S. Congress, 1973–2016. *Social Networks* 60 (Jan. 2020), 103–112. <https://doi.org/10.1016/j.socnet.2018.07.007>
- [37] Mark Newman. 2018. *Networks*. Vol. 1. Oxford University Press. <https://doi.org/10.1093/oso/9780198805090.001.0001>
- [38] Bogdan Nica. 2018. *A Brief Introduction to Spectral Graph Theory*. European Mathematical Society Publishing House, Zuerich, Switzerland. <https://doi.org/10.4171/188>
- [39] Lulu Pan, Haibin Shao, Mehran Mesbahi, Dewei Li, and Yugeng Xi. 2018. Structural Balance of Multiplex Signed Networks: A Distributed Data-Driven Approach. *Physica A: Statistical Mechanics and its Applications* 508 (Oct. 2018), 748–756. <https://doi.org/10.1016/j.physa.2018.05.101>
- [40] K. E. Read. 1954. Cultures of the Central Highlands, New Guinea. *Southwestern Journal of Anthropology* 10, 1 (April 1954), 1–43. <https://doi.org/10.1086/soutjanth.10.1.3629074>
- [41] Matthew Richardson, Rakesh Agrawal, and Pedro Domingos. 2003. Trust Management for the Semantic Web. In *The Semantic Web - ISWC 2003 (Lecture Notes in Computer Science)*, Dieter Fensel, Katia Sycara, and John Mylopoulos (Eds.). Springer, Berlin, Heidelberg, 351–368. https://doi.org/10.1007/978-3-540-39718-2_23

- [42] Majid Saberi, Reza Khosrowabadi, Ali Khatibi, Bratislav Misic, and Gholamreza Jafari. 2021. Topological Impact of Negative Links on the Stability of Resting-State Brain Network. *Scientific reports* 11, 1 (2021), 2176.
- [43] Hugo Saiz, Jesús Gómez-Gardeñes, Paloma Nuche, Andrea Girón, Yolanda Pueyo, and Concepción L. Alados. 2017. Evidence of Structural Balance in Spatial Ecological Networks. *Ecography* 40, 6 (June 2017), 733–741. <https://doi.org/10.1111/ecog.02561>
- [44] Samuel Franklin Sampson. 1968. *A Novitiate in a Period of Change: An Experimental and Case Study of Social Relationships*. Ph.D. Dissertation. Cornell University.
- [45] Simon Schweighofer, Frank Schweitzer, and David Garcia. 2020. A Weighted Balance Model of Opinion Hyper- Polarization. *Journal of Artificial Societies and Social Simulation* 23, 3 (2020), 5.
- [46] Ranveer Singh and Bibhas Adhikari. 2017. Measuring the Balance of Signed Networks and Its Application to Sign Prediction. *Journal of Statistical Mechanics: Theory and Experiment* 2017, 6 (June 2017), 063302. <https://doi.org/10.1088/1742-5468/aa73ef>
- [47] Lehoucq Sorensen, R. B. Lehoucq, and D. C. Sorensen. 1996. Deflation Techniques For An Implicitly Re-Started Arnoldi Iteration. *SIAM J. Matrix Anal. Appl.* 17, 4 (1996), 789–821.
- [48] Christoph Stadtfeld and Per Block. 2017. Interactions, Actors, and Time: Dynamic Network Actor Models for Relational Events. *Sociological Science* 4 (2017), 318–352. <https://doi.org/10.15195/v4.a14>
- [49] Szymon Talaga and Andrzej Nowak. 2022. Structural Measures of Similarity and Complementarity in Complex Networks. *Scientific Reports* 12, 1 (Oct. 2022), 16580. <https://doi.org/10.1038/s41598-022-20710-w>
- [50] Andreia Sofia Teixeira, Francisco C. Santos, and Alexandre P. Francisco. 2017. Emergence of Social Balance in Signed Networks. In *Complex Networks VIII*, Bruno Gonçalves, Ronaldo Menezes, Roberta Sinatra, and Vinko Zlatić (Eds.). Springer International Publishing, Cham, 185–192. https://doi.org/10.1007/978-3-319-54241-6_16
- [51] Leo Torres, Pablo Suárez-Serrato, and Tina Eliassi-Rad. 2019. Non-Backtracking Cycles: Length Spectrum Theory and Graph Mining Applications. *Applied Network Science* 4, 1 (Dec. 2019), 41. <https://doi.org/10.1007/s41109-019-0147-y>
- [52] Bahar Tunçgenç, Marwa El Zein, Justin Sulik, Martha Newson, Yi Zhao, Guillaume Dezechache, and Ophelia Deroy. 2021. Social influence matters: We follow pandemic guidelines most when our close circle does. *British Journal of Psychology* 112, 3 (2021), 763–780.
- [53] Nguyen Xuan Vinh, Julien Epps, and James Bailey. 2010. Information Theoretic Measures for Clusterings Comparison: Variants, Properties, Normalization and Correction for Chance. *The Journal of Machine Learning Research* 11 (2010), 2837–2854.
- [54] Stanley Wasserman and Katherine Faust. 1994. *Social Network Analysis: Methods and Applications*. Cambridge University Press, Cambridge; New York.

- [55] Robert B. Zajonc and Eugene Burnstein. 1965. Structural Balance, Reciprocity, and Positivity as Sources of Cognitive Bias. *Journal of Personality* 33, 4 (Dec. 1965), 570–583. <https://doi.org/10.1111/j.1467-6494.1965.tb01403.x>
- [56] Jing Zhang, Biao Liu, Jie Tang, Ting Chen, and Juanzi Li. 2013. Social influence locality for modeling retweeting behaviors. In *Twenty-third international joint conference on artificial intelligence*. Citeseer, 2761–2767.

Supplementary Information

S1. Proof of the existence of β_{\max} and related results

Using Eqs. (7) and (9) one can derive Eq. (3) as a weighted average of local balance:

$$\begin{aligned}
 K_S(G, \beta) &= \frac{\text{tr } \mathbf{W}_{k_0}^{k_1}(G, \beta)}{\text{tr } \mathbf{W}_{k_0}^{k_1}(|G|, \beta)} \\
 &= \frac{1}{\text{tr } \mathbf{W}_{k_0}^{k_1}(|G|, \beta)} \sum_{k=k_0}^{k_1} \frac{\beta^k}{k!} \text{tr } \mathbf{S}^k \\
 &= \sum_{k=k_0}^{k_1} \frac{\beta^k}{k!} \times \frac{\text{tr } |\mathbf{S}|^k}{\text{tr } \mathbf{W}_{k_0}^{k_1}(|G|, \beta)} \times \frac{\text{tr } \mathbf{S}^k}{\text{tr } |\mathbf{S}|^k} \\
 &= \sum_{k=k_0}^{k_1} C_{k_0}^{k_1}(G, \beta, k) K_S(G, k)
 \end{aligned} \tag{S1}$$

This result shows that global Balance Index, $K_S(G, \beta)$, is just a weighted average of local Balance Index values, $K_S(G, k)$, weighted by the corresponding contributions of semiwalks of different lengths. Now, contribution values are proportional to powers of β^k , namely, $C(G, \beta, k) \propto (\beta^k/k!) \text{tr } |\mathbf{S}|^k$, so in the limit as $\beta \rightarrow 0$ only the leading term $C(G, \beta, k_0) K_S(G, k_0)$ survives. Moreover, the same argument applies to any comparison between terms k and $k+1$ meaning that the locality principle can be always satisfied by choosing a sufficiently small β_{\max} . Hence, β_{\max} always exists. In particular, with sufficiently small β contribution arbitrarily close to 1 can be always assigned to the length $k = k_0$.

To strengthen the above argument we will now derive an analytic formula for approximating β_{\max} , which is quite accurate for graphs with large enough spectral gap, that is, the difference between largest and second largest eigenvalue. First, let us note that for the Locality Principle to hold, for all $k = k_0, \dots, k_1 - 1$ it must be true that:

$$\begin{aligned}
 &C_{k_0}^{k_1}(G, \beta, k) \geq C_{k_0}^{k_1}(G, \beta, k+1) \\
 \implies &\frac{\beta^k}{k!} \text{tr } |\mathbf{S}|^k \geq \frac{\beta^{k+1}}{(k+1)!} \text{tr } |\mathbf{S}|^{k+1} \\
 \implies &\sum_{i=1}^n \lambda_i^k \geq \frac{\beta}{k+1} \sum_{i=1}^n \lambda_i^{k+1}
 \end{aligned} \tag{S2}$$

where $\lambda_1 \geq \lambda_2 \geq \dots \geq \lambda_n$ are eigenvalues of $|\mathbf{S}|$ sorted in decreasing order. Now, since $|\mathbf{S}|$ is symmetric all its eigenvalues are real. Moreover by extended Perron-Frobenius theorem [38] λ_1 is always positive. Thus, the inequality in Eq. (S2), provided that the spectral gap $|\mathbf{S}|$ is large enough, can be simplified to:

$$\lambda_1^k \geq \frac{\beta}{k+1} \lambda_1^{k+1} \implies \beta \leq (k+1) \lambda_1^{-1} \tag{S3}$$

which gives the conditions for finding β_{\max} . Now, the last step is to realize that the above inequality holds for all k if and only if it holds for $k = k_0$. Hence:

$$\beta_{\max} \approx (k_0 + 1) \lambda_1^{-1} \tag{S4}$$

which serves as yet another evidence for the existence of β_{\max} .

S2. Proof of Theorem 4

We first prove necessity of the stated fact using a contradiction argument. Let G be a weakly balanced graph with i and j being a pair of nodes such that there is a semipath $p_{i \rightarrow j}$ with no negative edges between them and another semipath $q_{j \rightarrow i}$ with exactly one negative edge. Then, there is a cycle $(p_{i \rightarrow j}, q_{j \rightarrow i})$ with exactly one negative edge, so G is not weakly balanced by definition, which leads to a contradiction.

Now we show sufficiency. Let i and j be any two nodes connected by at least one all positive semipath. By hypothesis, such a pair cannot be simultaneously connected by a semipath with exactly one negative edge. As a result, G does not contain any semicycles with exactly one negative edge and is therefore weakly balanced.

S3. Computational complexity

Below are computation times for global, local and node-wise DoB measures for the three large networks studied in this paper (Epinions, Slashdot and Wikipedia). Performance was assessed using a laptop with AMD Ryzen 9 5900HX CPU and 16Gb of RAM. As evident in Fig. S1, all running times were arguably short. Global DoB and balance profiles were calculated in about 1 second or much less. Node-wise measures (for all nodes) were calculated in no more than 16 seconds (in the case of the largest network). All results include both the time needed for solving the eigenproblem(s), which can be cached and re-used in multiple computations, as well as any downstream computations using eigenvalues and eigenvectors. Furthermore, in all cases computation times seem to scale with respect to m in a very similar fashion with an average slope coefficient (in log-log scale) of about 0.61. This indicates that, at least for relatively low values of m , SWB computation times are only moderately (sub-linearly) affected when increasing the number of used leading eigenpairs.

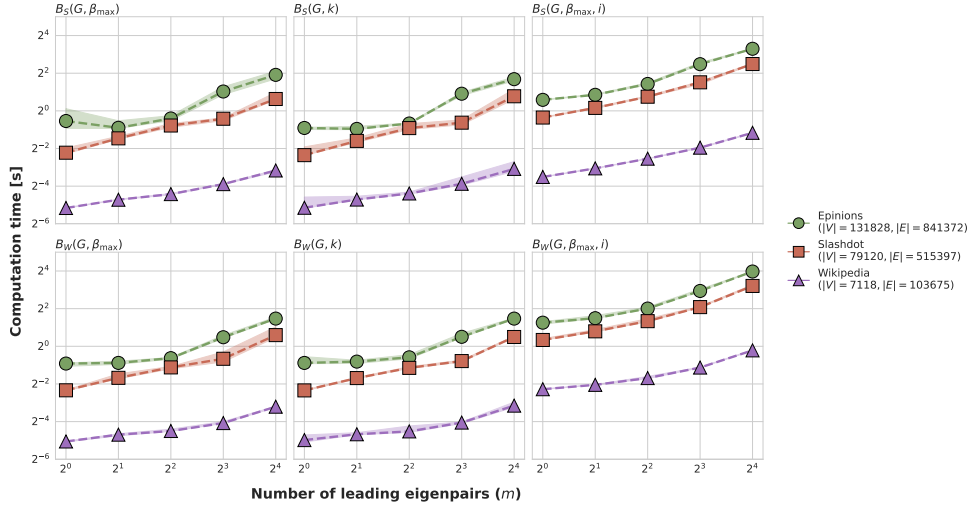


Figure S1. Running times of global, local and node-wise DoB measures (both strong and weak). Lines correspond to median times (over 10 repetitions) and bounds to 2nd and 9th deciles.

S4. Descriptive statistics for the U.S. Congress co-sponsorship networks

Chamber	Congress	f_R	f_D	$ V $	$ E $	f_+	B_S	B_W	\bar{d}	d_{cv}
House	93	0.43	0.56	446	18083	0.56	0.71	0.94	81.09	0.73
	94	0.33	0.67	445	19503	0.58	0.71	0.95	87.65	0.70
	95	0.34	0.66	444	21133	0.59	0.68	0.96	95.19	0.60
	96	0.38	0.62	442	51081	0.84	0.55	1.00	231.14	0.33
	97	0.45	0.54	447	49364	0.82	0.57	1.00	220.87	0.35
	98	0.39	0.61	444	48721	0.75	0.59	0.99	219.46	0.31
	99	0.42	0.57	443	49764	0.72	0.61	0.98	224.67	0.29
	100	0.42	0.58	446	50688	0.73	0.62	0.99	227.30	0.29
	101	0.42	0.58	449	56231	0.70	0.62	0.98	250.47	0.25
	102	0.40	0.60	447	58067	0.68	0.63	0.98	259.81	0.25
	103	0.42	0.58	446	59092	0.68	0.70	0.98	264.99	0.23
	104	0.53	0.46	445	62154	0.72	0.78	1.00	279.34	0.25
	105	0.52	0.48	449	66701	0.69	0.80	1.00	297.11	0.23
	106	0.51	0.49	442	63652	0.67	0.83	0.99	288.02	0.24
	107	0.51	0.48	447	63851	0.68	0.84	0.99	285.69	0.24
	108	0.52	0.47	444	66277	0.67	0.84	0.99	298.55	0.24
	109	0.53	0.47	445	66700	0.68	0.82	1.00	299.78	0.24
	110	0.46	0.54	452	70923	0.67	0.82	0.99	313.82	0.20
	111	0.41	0.59	451	70160	0.68	0.77	0.99	311.13	0.21
	112	0.54	0.45	450	77872	0.66	0.82	1.00	346.10	0.18
113	0.53	0.47	447	75771	0.64	0.86	1.00	339.02	0.18	
114	0.56	0.44	446	75180	0.65	0.86	1.00	337.13	0.19	
Senate	93	0.42	0.56	101	2439	0.76	0.62	0.99	48.30	0.35
	94	0.37	0.61	100	2432	0.79	0.63	1.00	48.64	0.35
	95	0.37	0.62	104	2336	0.81	0.57	1.00	44.92	0.39
	96	0.41	0.58	101	2275	0.82	0.55	1.00	45.05	0.39
	97	0.52	0.47	101	2073	0.79	0.60	0.99	41.05	0.37
	98	0.53	0.47	101	2194	0.76	0.58	0.99	43.45	0.33
	99	0.52	0.48	101	2177	0.75	0.61	0.99	43.11	0.33
	100	0.46	0.54	101	2143	0.72	0.60	0.99	42.44	0.36
	101	0.44	0.54	101	2445	0.68	0.63	0.98	48.42	0.31
	102	0.42	0.56	102	2479	0.71	0.64	0.99	48.61	0.31
	103	0.44	0.54	101	2257	0.72	0.70	0.99	44.69	0.35
	104	0.52	0.46	102	2324	0.74	0.81	1.00	45.57	0.38
	105	0.53	0.45	100	3002	0.70	0.81	1.00	60.04	0.27
	106	0.53	0.45	102	2930	0.72	0.78	0.99	57.45	0.25
	107	0.48	0.50	101	2522	0.73	0.70	0.99	49.94	0.30
	108	0.50	0.48	100	2387	0.74	0.79	0.99	47.74	0.28
	109	0.53	0.45	101	2823	0.73	0.82	0.99	55.90	0.25
	110	0.49	0.49	102	2779	0.70	0.85	0.99	54.49	0.30
	111	0.39	0.59	109	3645	0.74	0.68	1.00	66.88	0.27
	112	0.48	0.50	101	3914	0.69	0.78	1.00	77.50	0.20
113	0.44	0.54	105	3932	0.65	0.86	1.00	74.90	0.24	
114	0.54	0.44	100	3696	0.61	0.96	1.00	73.92	0.20	

f_R, f_D – fraction of Republicans/Democrats (may not sum up to 1 due to the presence of other parties and/or independents)

$|V|, |E|$ – number of nodes/edges

f_+ – fraction of positive edges

B_S, B_W – strong/weak degree of balance

\bar{d}, d_{cv} – average degree and coefficient of variation of degree distribution